C.P. No.1393

C.P. No.1393

PROCUREMENT EXECUTIVE, MINISTRY OF DEFENCE

Aeronautical Research Council
Current Papers

THE CALCULATION, BY A FINITE-DIFFERENCE METHOD, OF SUBCRITICAL FLOW WITHOUT CIRCULATION PAST A SWEPT ELLIPTIC CYLINDER BETWEEN WALLS

by

G.J. Clapworthy

Aerodynamics Dept., RAE Farnborough, Hants

£2 NET

London: Her Majesty's Stationery Office

*C.P. No.1393
June 1976

THE CALCULATION, BY A FINITE-DIFFERENCE METHOD, OF SUBCRITICAL FLOW WITHOUT CIRCULATION PAST A SWEPT ELLIPTIC CYLINDER BETWEEN WALLS

by

G. J. Clapworthy**
Aerodynamics Department, RAE Farnborough, Hants

SUMMARY

The full equations of motion are expressed in coordinates defined by the body shape and the exact body surface boundary conditions are applied. The flow equations are expressed in terms of the velocity potential and are solved by finite-difference methods. For accuracy, further transformations are necessary to concentrate the grid points in regions of greatest variation in potential.

Mach number and pressure distributions are presented for typical cases.

This work was done under the link between the University of Southampton and the RAE

---

* Replaces RAE Technical Report 76074 - ARC 37032

** Now at the Polytechnic of North London, Holloway, London, N7 8DB

LIST OF CONTENTS

1 INTRODUCTION

Reliable methods for the numerical calculation of two-dimensional, subcritical, potential flows past general shapes (lifting and non-lifting) have been available for some years, notably the work of Sells[1]. Subsequent work dealt with plane supercritical flows, some of the more important work being done by Murman and Cole[2] in small perturbation theory, and Steger and Lomax[3] and Bauer, Garabadian and Korn[4] who considered the full equations of motion. The usual method of solution was by finite differences, using central differences in subcritical regions and backward differences in the supercritical zones.

Improvements in computer hardware have made it feasible to attempt the calculation of flows around three-dimensional bodies. The method normally used has been transonic small-perturbation theory and examples of the solution of the full equations of motion, applying the boundary conditions exactly, have been few, *eg* Duck[5], Jameson[6].

This Report deals with a numerical scheme to calculate the steady, subcritical flow around a swept elliptic cylinder between walls. The full equation of motion is expressed in terms of the velocity potential and is solved using the exact body surface boundary conditions. The speed of sound is obtained from Bernoulli's equation.

The work is done in coordinates defined by the body shape, thus allowing the boundary conditions to be satisfied in a straightforward manner. The infinite flow field is mapped into a finite region by means of a transformation of one of the variables. For an accurate solution, further transformations of the other two variables are necessary to concentrate the grid points in regions of greatest change in potential.

Section 2 gives details of the transformations used to reach the final coordinate system in which we express the equations of motion (section 3). Details of the computation are given in section 4 followed, in section 5, by the results. The concluding remarks appear in section 6. Details of the derivation of terms required in the continuity equation are given in Appendix A and Appendix B deals with the matrix inversion technique used.

2 THE COORDINATE SYSTEM

Our original cartesian coordinate system, x^i, is defined with the stream flowing in the $-x^2$ direction, x^3 being vertically upward and the walls being given by $x^1 = \pm s$ (see Fig.1). This notation enables us to describe our transformations succinctly using tensor analysis. The conventional (x,y,z) system is equivalent to $(-x^2, x^1, x^3)$.

We transform to a non-orthogonal reference system, ξ^i, as described in section 5 of Mangler and Murray[7]. The walls and planes parallel to them are represented by $\xi^1 =$ constant and the cylinder is represented by $\xi^2 = 0$. The system is chosen such that the base vectors $\underline{a}_2$ and $\underline{a}_3$ (see Appendix A) are perpendicular to each other and normal to the x^1-axis (i.e. y-axis). This transformation is equivalent to conformal mappings in the set of cross-sectional planes $x^1 =$ constant. We are concerned with an untapered cylinder, in which case $\underline{a}_1$ will be parallel with the leading edge ($\xi^2 = 0$, $\xi^3 = 0$), which is swept by an angle Λ (see Fig.1).

For an untapered cylinder the mapping has the general form

$$x^1 = \xi^1 ; \qquad x^2 + ix^3 = -\mu\xi^1 + f(\zeta) , \tag{2-1}$$

[i.e. $y = \xi^1$; $-x + iz = -\mu\xi^1 + f(\zeta)$]

where
$$\zeta = \xi^2 + i\xi^3 , \tag{2-2}$$

and
$$\mu = \tan\Lambda .$$

For a wing whose profile in the cross-sectional planes is the ellipse defined by

$$\frac{(\mu x^1 + x^2)^2}{c^2} + \frac{(x^3)^2}{c^2\tau^2} = 1 , \tag{2-3}$$

where c is the semi-chord and τ is the thickness parameter in the cross-sectional plane, the mapping function is defined by

$$f(\zeta) = c\cosh\zeta + c\tau\sinh\zeta . \tag{2-4}$$

The limits of the coordinates are

$$-s \leqslant \xi^1 \leqslant s ; \qquad 0 \leqslant \xi^2 \leqslant \infty ; \qquad 0 \leqslant \xi^3 \leqslant 2\pi \ .$$

Since we are dealing with the non-lifting case we can make use of the symmetry about the plane $x^3 = 0$ to reduce our considerations to $x^3 \geqslant 0$ only. This reduces the range of ξ^3 to $0 \leqslant \xi^3 \leqslant \pi$, where ($\xi^2 = 0$, $\xi^3 = \pi$) represents the trailing edge.

The transformation defined in (2-1) trivially satisfies the integrability condition given in Ref 7.

Let

$$\frac{df}{d\zeta} = C + iD ; \qquad \left|\frac{df}{d\zeta}\right| = A \ , \tag{2-5}$$

so that

$$A^2 = C^2 + D^2 \ . \tag{2-6}$$

From these equations we derive, in Appendix A, relationships which are required in the equations of motion.

For an elliptic cylinder

$$C = \tfrac{1}{2}c\left[(1+\tau)e^{\xi^2} - (1-\tau)e^{-\xi^2}\right] \cos \xi^3 \tag{2-7}$$

$$D = \tfrac{1}{2}c\left[(1+\tau)e^{\xi^2} + (1-\tau)e^{-\xi^2}\right] \sin \xi^3 \ . \tag{2-8}$$

For the application of finite difference methods to the equations of motion, further transformations are necessary. To shrink the infinite range of ξ^2 to a finite working space, we define

$$\eta^2 = 1 - e^{-\xi^2} ; \qquad 0 \leqslant \eta^2 \leqslant 1 \tag{2-9}$$

and to concentrate the grid points in areas of greatest change in velocity potential, we apply the transformations

$$\eta^1 = \frac{\xi^1}{\sqrt{(\alpha+1)s^2 - \alpha(\xi^1)^2}} ; \qquad \eta^3 = \frac{2(\xi^3 - \tfrac{1}{2}\pi)}{\sqrt{(\beta+1)\pi^2 - 4\beta(\xi^3 - \tfrac{1}{2}\pi)^2}} \ , \tag{2-10}$$

where $-1 \leqslant \eta^1, \eta^3 \leqslant 1$

and $0 \leqslant \alpha, \beta < \infty$.

The η^3-transformation is applicable only to the non-lifting case where we use the range $0 \leqslant \xi^3 \leqslant \pi$.

In equation (2-10) α and β are parameters to adjust the transformation as required. The effect of increasing α is to bunch grid points near the walls, and increasing β similarly bunches points at the leading and trailing edges. This is illustrated in Fig.2. If the parameter is zero in either case, the transformation merely represents a scaling. The practical ranges of α and β depend upon the particular configuration being investigated, for example, if the span is increased then α must also be increased to maintain the fineness of the mesh near the walls, which is where the greatest variations occur.

In the equations of motion we will require the derivatives of transformations (2-9) and (2-10), denoted by $P_i = d\eta^i/d\xi^i$, and these are

$$P_1 = \frac{\Delta^{3/2}}{s\sqrt{\alpha + 1}} ; \qquad P_2 = 1 - \eta^2 ; \qquad P_3 = \frac{2\Gamma^{3/2}}{\pi\sqrt{\beta + 1}} \tag{2-11}$$

where $$\Delta = \alpha(\eta^1)^2 + 1 , \qquad \Gamma = \beta(\eta^3)^2 + 1 . \tag{2-12}$$

3 THE EQUATIONS OF MOTION AND BOUNDARY CONDITIONS

If we denote the velocity vector by $\underline{V}$ and the velocity potential by Φ , then the contravariant and covariant components of velocity will be V^i and V_i respectively, where

$$V^i = \underline{V} \cdot \underline{a}^i ; \qquad V_i = \underline{V} \cdot \underline{a}_i = \frac{\partial \Phi}{\partial \xi^i} . \tag{3-1}$$

The relations between these quantities are set out in Appendix A and if the speed $|\underline{V}|$ is denoted by q , equation (A-17) gives

$$q^2 = V^i V_i = g^{ij} V_i V_j . \tag{3-2}$$

Mangler and Murray[2] derive the equation of continuity for a compressible inviscid fluid in steady irrotational motion with no external forces in the form:

$$\frac{1}{J}\frac{\partial}{\partial \xi^i}(JV^i) - \frac{V^i}{2a^2}\frac{\partial}{\partial \xi^i}(q^2) = 0 \quad , \tag{3-3}$$

where J is as defined in equation (A-1) and a is the local speed of sound obtained from Bernoulli's equation:

$$\frac{a^2}{\gamma - 1} + \tfrac{1}{2}q^2 = \text{constant} \quad . \tag{3-4}$$

Here γ is the ratio of specific heats.

The freestream velocity potential is given by

$$\Phi_\infty = -U_\infty x^2 \quad , \tag{3-5}$$

since the stream is in the negative x^2-direction.

We express equation (3-3) in terms of the perturbation velocity potential

$$\phi = \Phi - \Phi_\infty = \Phi + U_\infty x^2 = \Phi + U_\infty[-\mu\xi^1 + \mathrm{Re}(f)] \quad , \tag{3-6}$$

and non-dimensionalise with respect to U_∞ and c.

Using equation (A-11), we define a set of coefficients, Q^i, by

$$Q^i = \frac{1}{J}\frac{\partial}{\partial \xi^j}(Jg^{ij}) = \frac{1}{A^2}\frac{\partial}{\partial \xi^j}[A^2 g^{ij}] \quad . \tag{3-7}$$

These arise when we expand the first term in equation (3-3):

$$\frac{1}{J}\frac{\partial}{\partial \xi^i}(JV^i) = g^{ij}\frac{\partial^2 \Phi}{\partial \xi^i \partial \xi^j} + Q^i\frac{\partial \Phi}{\partial \xi^i} \quad .$$

We find that $Q^1 \equiv 0$.

The second term in equation (3-3) is similarly expanded. If, for clarity, we denote V^i by Y_i then, after lengthy algebra, equation (3-3) when expressed in terms of the perturbation potential with respect to the η^i system of coordinates, becomes

$$\left(1 - \frac{Y_1^2}{a^2}\right) P_1^2 \phi_{11} + \left(\frac{A^2 + \mu^2 C^2}{A^4} - \frac{Y_2^2}{a^2}\right) P_2^2 \phi_{22} + \left(\frac{A^2 + \mu^2 D^2}{A^4} - \frac{Y_3^2}{a^2}\right) P_3^2 \phi_{33}$$

$$= -2\left(\frac{\mu C}{A^2} - \frac{Y_1 Y_2}{a^2}\right) P_1 P_2 \phi_{12} + 2\left(\frac{\mu D}{A^2} + \frac{Y_1 Y_3}{a^2}\right) P_1 P_3 \phi_{13}$$

$$+ 2\left(\frac{\mu^2 CD}{A^4} + \frac{Y_2 Y_3}{a^2}\right) P_2 P_3 \phi_{23} + \left(\frac{Y_1^2}{a^2} - 1\right) \frac{3\alpha\eta^1 \Delta^{\frac{1}{2}}}{s\sqrt{\alpha + 1}} P_1 \phi_1$$

$$+ \left[\left(\frac{A^2 + \mu^2 C^2}{A^4} - \frac{Y_2^2}{a^2}\right) + \left(\frac{Y_1^2}{a^2} - 1\right) Q^2\right] P_2 \phi_2$$

$$- \left[\left(\frac{A^2 + \mu^2 D^2}{A^4} - \frac{Y_3^2}{a^2}\right) \frac{6\beta\eta^3 \Gamma^{\frac{1}{2}}}{\pi\sqrt{\beta + 1}} - \left(\frac{Y_1^2}{a^2} - 1\right) Q^3\right] P_3 \phi_3$$

$$+ \left(\frac{V_3^2 - V_2^2}{A^4 a^2}\right) E + \frac{2V_2 V_3}{A^4 a^2} F + \frac{2\mu Y_1 T}{A^2 a^2} \left(V_2^2 + V_3^2\right)$$

$$- \frac{(RV_2 + SV_3)}{a^2} \left[2\mu Y_1 + \frac{V_2^2 + V_3^2}{A^2}\right] , \qquad (3\text{-}8)$$

where $$\phi_{ij} = \frac{\partial^2 \phi}{\partial \eta^i \partial \eta^j} ; \quad \phi_i = \frac{\partial \phi}{\partial \eta^i} ; \quad \frac{d^2 f}{d\zeta^2} = E + iF ; \qquad (3\text{-}9)$$

$$R = \frac{CE + DF}{A^4} ; \quad S = \frac{DE - CF}{A^4} ; \quad T = DS - CR . \qquad (3\text{-}10)$$

The boundary conditions to be applied are those of tangential flow at the boundaries. Since $\underline{a}^i$ is normal to the surface ξ^i = constant , the tangential flow condition on that surface ($\underline{V} \cdot \underline{a}^i = 0$) implies, from equation (A-16), that $V^i = 0$.

The boundary conditions are:

(i) <u>on the body surface $\eta^2 = 0$,</u>

$$V^2 = g^{2i} \frac{\partial \Phi}{\partial \xi^i} = 0$$

which becomes, using equations (2-5), (2-11), (3-6), (3-9) and (A-12),

$$\frac{\mu C}{A^2} P_1\phi_1 + \frac{A^2 + \mu^2 C^2}{A^4} \phi_2 - \frac{\mu^2 CD}{A^4} P_3\phi_3 = \frac{C}{A^2} \quad ; \tag{3-11}$$

(note that on the body $P_2 = 1$).

(ii) <u>on the walls $\eta^1 = \pm 1$</u>,

by similar algebra,

$$P_1\phi_1 + \frac{\mu C}{A^2} P_2\phi_2 - \frac{\mu D}{A^2} P_3\phi_3 = 0 \quad ; \tag{3-12}$$

(iii) <u>at the wall-body junction</u>,

since equations (3-11) and (3-.2) must be satisfied simultaneously,

$$\phi_2 = C \quad ; \qquad P_1\phi_1 - \frac{\mu D}{A^2} P_3\phi_3 = - \frac{\mu C^2}{A^2} \quad ; \tag{3-13}$$

(iv) <u>at infinity, $\eta^2 \to 1$</u>,

$$\phi \to 0 \quad . \tag{3-14}$$

Equation (3-8) and boundary conditions (3-11) to (3-14) are expressed in finite difference form as outlined in section 4. As stated previously, the symmetry of the flow enables us to restrict computation to the upper half of the flow field to save on computer time and storage. Also, for profiles with fore-and-aft symmetry, such as the ellipse, we can exploit the antisymmetry in ϕ, i.e.

$$\phi(\eta^1,\eta^2,\eta^3) = - \phi(-\eta^1,\eta^2,-\eta^3) \quad , \tag{3-15}$$

further to reduce the computation.

4 DETAILS OF THE COMPUTATION

The differencing scheme applied to equation (3-8) was the usual central differences approach in which, for example,

$$\frac{\partial\phi}{\partial\eta^1} = \frac{\phi_{i+1,j,k} - \phi_{i-1,j,k}}{2h_1} + O\left(h_1^2\right) \tag{4-1}$$

$$\frac{\partial^2\phi}{(\partial\eta^3)^2} = \frac{\phi_{i,j,k+1} - 2\phi_{i,j,k} + \phi_{i,j,k-1}}{(h_3)^2} + O\left(h_3^2\right) \qquad (4\text{-}2)$$

$$\frac{\partial^2\phi}{\partial\eta^1\partial\eta^2} = \frac{\phi_{i+1,j+1,k} - \phi_{i+1,j-1,k} - \phi_{i-1,j+1,k} + \phi_{i-1,j-1,k}}{4h_1h_2} + O\left(h_1^2 + h_2^2\right) \qquad (4\text{-}3)$$

where h_i is the step-length in η^i and $\phi_{i,j,k}$ is the value of ϕ at the (i,j,k)th grid point in η^1, η^2, η^3 respectively. The port wall corresponds to $i = 1$, the body to $j = 1$ and the leading edge to $k = 1$.

The only exception is at the wall-body junction for the calculation of $\frac{\partial^2\phi}{\partial\eta^1\partial\eta^2}$ (see Fig.3). To apply formula (4-3) at point (1,1,k), we require $\phi_{0,0,k}$ which is not obtainable from the boundary conditions. We therefore resort to the formula

$$\frac{\partial^2\phi}{\partial\eta^1\partial\eta^2} = \frac{1}{2h_1h_2}\left[\phi_{2,1,k} + \phi_{0,1,k} + \phi_{1,2,k} + \phi_{1,0,k} - 2\phi_{1,1,k} - \phi_{0,2,k} - \phi_{2,0,k}\right] + O\left(h_1^2 + h_2^2\right) . \qquad \ldots\ldots (4\text{-}4)$$

The second, fourth, sixth and seventh terms are calculated from the boundary conditions, that is, by applying, respectively, the finite-difference forms of equation (3-13b) at point (1,1,k), of equation (3-13a) at point (1,1,k), of (3-12) at (1,2,k) and of (3-11) at (2,1,k).

The error term in equation (4-4) is different from that of equation (4-3), though of the same order.

Having differenced equation (3-8) as above, the equation is arranged as suggested by Sells[1] to give a tridiagonal matrix which is solved by block relaxation. We can solve in two different ways: on lines η^2 = constant (rings) and on lines η^3 = constant (spokes). The forms of the equations are:

rings: $\quad d_k\phi_{i,j,k-1} + c_k\phi_{i,j,k} + b_k\phi_{i,j,k+1} = a_k , \qquad 1 \leqslant k \leqslant L ,$

spokes: $\quad d_j\phi_{i,j-1,k} + c_j\phi_{i,j,k} + b_j\phi_{i,j+1,k} = a_j , \qquad 1 \leqslant j \leqslant M .$

Application of the symmetry condition at the leading and trailing edges in the rings example means that $d_1 = b_L = 0$. Application of the body surface condition and the condition at infinity ($\eta^2 \to 1$) in the spokes case means that $d_1 = b_M = 0$. Thus in both cases the matrices are wholly tridiagonal and do not have the corner elements present in Sells' work. This makes the matrix inversion somewhat simpler; details are presented in Appendix B.

In the cases of both rings and spokes the field is swept first in the cross-sectional plane and subsequently by moving the plane from the port wall through the field.

5 RESULTS

In Figs.4 to 7 we present results for a flow with freestream Mach number 0.65 past an elliptic cylinder swept at an angle of 45^o. The aspect ratio is 2 and the thickness/chord ratio, τ , is 0.1. This case exhibits the typical properties of the flows considered.

Fig.4 shows the chordwise distribution of local Mach number at several sections. It is observed that at the port wall ($y = -s$) there is a high peak with large gradients in the neighbourhood of the trailing edge. This arises from the combined effects of the sweep, which accelerates the flow normal to the leading edge, the constraint of the wall and the rapidly increasing slope of the profile in this region. It is shown in greater detail in Fig.5. By the anti-symmetry, there is a similar peak near the leading edge of the starboard wall. The distribution in the centre section is almost indistinguishable from that for the infinite swept wing with the walls absent.

Fig.6 shows the local Mach number distributions in sections parallel to the leading edge. We see that the behaviour in the centre of the span is very smooth and that the peak extends only a small distance from the wall.

Fig.7 shows a plan of Mach number contours on the wing surface and emphasizes the local nature of the peak. Fig.8 shows a magnified view of the trailing edge region of Fig.7.

The Mach contours meet the wall normally and there are occasions when lines of constant chord cross and then recross them. This explains the occurrence of the depressions in curves 6 and 7 of Fig.6 and the slight lip in curve 4. The phenomenon is best observed in Fig.8 near the junction of the wall and the 0.81 contour. This is close to the chordwise station for curve 4.

By considering the starboard wall, it can be seen that at the centre of a swept-forward wing there will be a pressure peak near the leading edge, even for a profile section.

Fig.9a to 9d for the same wing are included to show the variation of the pressure distribution as the freestream Mach number increases through 0.1, 0.45 and 0.6 to 0.65. There is relatively little change in the pressure at the centre span but close to the wall the peak becomes much more exaggerated. The position and magnitude of minimum pressure is marked in each case with a cross, and the adjacent numeral shows the peak Mach number.

Other calculations have shown that curves of local Mach number for lower values of M_∞ have the same form as in Figs.4 and 6 but exhibit lower 'plateaux' and have relatively smaller peaks. An increase in the span appears fractionally to decrease the height of the peak while a reduction in the angle of sweep decreases the peakiness and shifts the peak forward marginally.

In a typical run, the computation is started on a coarse grid (11 × 6 × 11 in η^1, η^2, η^3 respectively) and a mesh-halving routine is implemented twice to reach a final grid of 41 × 24 × 41. The program stops when the change in potential from one iteration to the next is less (at all grid points) than some prescribed value. For a change in potential of less than 10^{-5} per iteration (corresponding to a change in Mach number of 3×10^{-5} per iteration), we require 100 iterations on the finest grid, following 250 and 200 respectively on the coarse grids. Total computation time on a CDC 7600 computer is approximately 270 seconds. For a change in potential of less than 2×10^{-6} per iteration (corresponding to a Mach number change of 3×10^{-6} per iteration), we require 350 iterations on the finest grid and the computation time increases to 700 seconds. The relaxation parameters used - ω in equation (B-4) - are 1.83 for the first mesh size and 1.84 for the subsequent grids.

The convergence appears to be rather sensitive to the choice of transformation parameters, α and β. For the case studied in detail, results obtained for different values of α and β lying between 5 and 15 were consistent, apart from at the apex of the peak where there was a range of disagreement of 1 to 2%, because of the impossibility of placing sufficient points in this region for a practical size of grid. If the parameters lay outside this range, then the grid points were either spread too thinly near the walls and the leading and trailing edges to deal numerically with the 'peaking', or they were so bunched in these

areas that the remainder of the field was underpopulated. In these situations, the solutions were not wholly reliable, or worse, there was a tendency for the solutions to diverge for the small grid sizes, causing the computation eventually to break down. In this context, decreasing the relaxation parameter may help if the divergence is not too rapid, at the cost of increased computation time.

It should be noted that the working range of the parameters given above is not absolute and will be different for different wing geometries - the important point is to maintain the density of points near the peak. If the span is doubled, for example, one would have to increase α , probably to within the range 12 to 25.

Tables 2 to 5 contain values for the perturbation velocity potential at a selection of grid points as an aid to future investigators. The total velocity potential can be calculated using equation (3-5) in conjunction with equations (2-1), (2-4), (2-9) and (2-10). Values of the constants are $\Lambda = 45^{\circ}$, $\tau = 0.1$, $M_{\infty} = 0.65$, $\alpha = 11$, $\beta = 8$, the grid sizes in ξ^1, ξ^2, ξ^3 being $41 \times 25 \times 61$. The data are shown for four sectional planes, at alternative points along alternate spokes (reading horizontally). Note that the tabulated values are $10 \times \phi$ for convenience.

Calculations have been made for the geometries and Mach numbers listed in Table 1. Further details of these results can be obtained from the author at the Department of Mathematics, Polytechnic of North London, Holloway, London, N7 8DB.

Table 1

SUMMARY OF RESULTS OBTAINED

Aspect ratio	Thickness, τ	Sweep, Λ°	Mach No., M_{∞}
2.0	0.1	45	0.65
2.0	0.1	45	0.6
2.0	0.1	45	0.5
2.0	0.1	45	0.45
2.0	0.1	45	0.1
2.0	0.1	30	0.6
2.0	0.1	20	0.6
4.0	0.1	45	0.6

6 CONCLUDING REMARKS

Results have been obtained for subcritical flow past swept elliptic cylinders between walls. The full equation of motion was expressed in terms of non-orthogonal coordinates defined by the body shape and the boundary conditions were thus satisfied exactly. The equation was solved using finite differences.

The method is at present being extended to deal with different profiles, such as the Karman-Trefftz, and to cover the case of a semi-infinite swept wing. It is hoped to deal also with supercritical flows.

Acknowledgments

The author would like to express his gratitude to Prof. K.W. Mangler for his help at all stages of this work. Thanks are due also to the SRC for giving financial support to this work.

Appendix A

SOME RELATIONS FROM TENSOR CALCULUS

If we have a transformation from a cartesian coordinate system, x^i , to a general system of coordinates, ξ^j , of the form

$$x^i = x^i(\xi^1,\xi^2,\xi^3) \quad ; \qquad i = 1,2,3$$

the Jacobian of the transformation, denoted J , is given by

$$J = \left| \frac{\partial x^i}{\partial \xi^j} \right| \quad , \tag{A-1}$$

where $J \neq 0$ except, perhaps, at isolated singular points.

At each point we construct a system of base vectors, $\underline{a}_i$, $i = 1, 2, 3$, which are tangential to the curves of intersection of the surfaces ξ^{i-1} = constant and ξ^{i+1} = constant . We also construct a set of vectors, $\underline{a}^i$, normal to the surfaces ξ^i = constant . Employing the summation convention of tensor analysis, we relate the vectors by

$$J\varepsilon_{ijk}\underline{a}^i = \underline{a}_j \times \underline{a}_k \quad , \tag{A-2}$$

where $\varepsilon_{ijk} = \begin{cases} +1 \text{ if } i, j, k \text{ are an even permutation of } 1, 2, 3 \\ -1 \text{ if } i, j, k \text{ are an odd permutation of } 1, 2, 3 \\ 0 \text{ otherwise} \end{cases}$

We define a tensor, t , by

$$dx^i = \frac{\partial x^i}{\partial \xi^j} d\xi^j \equiv t^i_j d\xi^j \quad . \tag{A-3}$$

It can be shown that if $\underline{c}_i$ are the cartesian unit base vectors, then

$$\underline{a}_j = t^i_j \underline{c}_i \quad . \tag{A-4}$$

We define the symmetric covariant metric tensor, g_{ij} , and the contravariant metric tensor, g^{ij} , by

$$g_{ij} = \underline{a}_i \cdot \underline{a}_j \quad ; \qquad g^{ij} = \underline{a}^i \cdot \underline{a}^j \quad . \tag{A-5}$$

Since

$$\underline{c}_r \cdot \underline{c}_s = \delta_{rs} = \begin{cases} 1 \text{ if } r = s \\ 0 \text{ if } r \neq s \end{cases} ,$$

equations (A-4) and (A-5) give

$$g_{ij} = t_i^s t_j^r \delta_{rs} . \tag{A-6}$$

This property can be used to show

$$\underline{a}_i = g_{ij} \underline{a}^j , \tag{A-7}$$

$$\underline{a}^j = g^{jk} \underline{a}_k , \tag{A-8}$$

$$g_{ij} g^{jk} = \delta_i^k , \tag{A-9}$$

where δ_i^k is defined similarly to δ_{rs} .

The system of equations (A-9) can be solved for g^{in} ,

$$\varepsilon_{ijk} J^2 g^{in} = \varepsilon^{nrs} g_{jr} g_{ks} , \tag{A-10}$$

with ε^{nrs} defined as ε_{ijk} previously.

Hence, given the form of the transformation as in (2-1) and (2-4), we can use equation (A-3) to calculate t_j^i and use (A-6) then to calculate g_{ij} . Equation (A-10) used in conjunction with equation (A-1) now gives g^{ij} .

For transformations of the general form of equation (2-1) we obtain, using equations (2-5) and (2-6),

$$J = A^2 , \tag{A-11}$$

and

$$\left[g^{ij}\right] = \begin{bmatrix} 1 & \frac{\mu C}{A^2} & -\frac{\mu D}{A^2} \\ \frac{\mu C}{A^2} & \frac{A^2 + \mu^2 C^2}{A^4} & -\frac{\mu^2 CD}{A^4} \\ -\frac{\mu D}{A^2} & -\frac{\mu^2 CD}{A^4} & \frac{A^2 + \mu^2 D^2}{A^4} \end{bmatrix} . \tag{A-12}$$

For the particular case of the elliptic section we substitute for C and D from equations (2-7) and (2-8).

Any vector $\underline{v}$ can be written in the forms

$$\underline{v} = v_i \underline{a}^i = v^j \underline{a}_j \quad , \tag{A-13}$$

where v_i, v^j are respectively the covariant and contravariant components of $\underline{v}$.

From equations (A-5), (A-7) and (A-9)

$$\underline{a}_i \cdot \underline{a}^k = g_{ij} \underline{a}^j \cdot \underline{a}^k = \delta_i^k \tag{A-14}$$

Thus using equations (A-5), (A-13) and (A-14),

$$v_i = \underline{v} \cdot \underline{a}_i = g_{ij} v^j \quad . \tag{A-15}$$

Similarly,

$$v^i = \underline{v} \cdot \underline{a}^i = g^{ij} v_j \quad . \tag{A-16}$$

Using equations (A-13), (A-14) and (A-16) we find

$$|\underline{v}|^2 = \underline{v} \cdot \underline{v} = v_i v^j \underline{a}^i \cdot \underline{a}_j \quad ,$$

i.e.

$$|\underline{v}|^2 = v_i v^i = g^{ij} v_i v_j \quad . \tag{A-17}$$

Appendix B

MATRIX INVERSION

We solve explicitly the rings example. The matrix equation is of the form $Tu = a$ where

$$T = \begin{bmatrix} c_1 & b_1 & & & & \\ d_2 & c_2 & b_2 & & \bigcirc & \\ & d_3 & c_3 & b_3 & & \\ & & & \ddots & \ddots & \ddots \\ \bigcirc & & & d_{L-1} & c_{L-1} & b_{L-1} \\ & & & & d_L & c_L \end{bmatrix}$$

and $u_k = \phi^{(n+1)}_{i,j,k}$ for fixed i, j , the superscript referring to the value at the $(n + 1)$th iteration.

The matrix T is now factorised into upper and lower triangular matrices so that

$$T = RU \quad . \tag{B-1}$$

Here,

$$R = \begin{bmatrix} r_1 & & & & \\ s_2 & r_2 & & \bigcirc & \\ & s_3 & r_3 & & \\ & & \ddots & \ddots & \ddots \\ \bigcirc & & s_{L-1} & r_{L-1} & \\ & & & s_L & r_L \end{bmatrix}; \quad U = \begin{bmatrix} 1 & x_1 & & & \\ & 1 & x_2 & \bigcirc & \\ & & 1 & x_3 & \\ & & & \ddots & \ddots \\ \bigcirc & & & 1 & x_{L-1} \\ & & & & 1 \end{bmatrix}$$

If R is non-singular and

$$z = Uu = R^{-1}a \quad ,$$

our problem is equivalent to solving successively

$$Rz = a \ , \tag{B-2}$$

$$Uu = z \ . \tag{B-3}$$

Thus we obtain the following sets of equations from (B-1) and (B-2)

$$\left.\begin{aligned} d_k &= s_k \\ c_k &= s_k x_{k-1} + r_k \\ b_k &= r_k x_k \\ a_k &= s_k z_{k-1} + r_k z_k \end{aligned}\right\} \ 2 \leqslant k \leqslant L \ .$$

In this scheme x_k and z_k are calculated without the need to store r_k, s_k . We now use equation (B-3) to obtain

$$u_L = z_L \ ,$$

$$u_k = z_k - x_k u_{k+1} \ , \qquad L - 1 \geqslant k \geqslant 1 \ .$$

The matrix u is calculated in reverse order.

If we require over- or under-relaxation, we then put

$$\phi_{i,j,k}^{(n+1)} = \omega u_k + (1 - \omega)\phi_{i,j,k}^{(n)} \tag{B-4}$$

where ω is the relaxation parameter and the superscript $(n + 1)$ refers to the updated value of $\phi_{i,j,k}$.

The procedure for solution along spokes is identical.

Table 2

VALUES OF PERTURBATION POTENTIAL × 10 IN PLANE $x^1 = -s$ (WALL)

Body ⟶ ∞

	ξ^3/π \ ξ^2	0	0.0870	0.1823	0.2877	0.4055	0.5390	0.6931	0.8755	1.0986	1.3863	1.7918	2.4849
ℓ.e.	0	-0.7496	-0.6887	-0.6292	-0.5680	-0.5060	-0.4436	-0.3815	-0.3194	-0.2581	-0.1979	-0.1386	-0.0778
	0.0041	-0.7498	-0.6888	-0.6293	-0.5680	-0.5060	-0.4437	-0.3815	-0.3194	-0.2581	-0.1979	-0.1386	-0.0778
	0.0090	-0.7508	-0.6895	-0.6296	-0.5682	-0.5062	-0.4438	-0.3814	-0.3194	-0.2581	-0.1979	-0.1386	-0.0778
	0.0149	-0.7529	-0.6904	-0.6304	-0.5687	-0.5065	-0.4440	-0.3816	-0.3195	-0.2582	-0.1979	-0.1386	-0.0778
	0.0223	-0.7567	-0.6926	-0.6318	-0.5697	-0.5072	-0.4444	-0.3819	-0.3197	-0.2583	-0.1980	-0.1386	-0.0778
	0.0315	-0.7628	-0.6964	-0.6343	-0.5714	-0.5083	-0.4453	-0.3824	-0.3201	-0.2585	-0.1981	-0.1386	-0.0778
	0.0431	-0.7721	-0.7028	-0.6385	-0.5743	-0.5104	-0.4467	-0.3834	-0.3207	-0.2589	-0.1983	-0.1387	-0.0778
	0.0580	-0.7856	-0.7127	-0.6459	-0.5792	-0.5138	-0.4491	-0.3851	-0.3218	-0.2596	-0.1987	-0.1389	-0.0778
	0.0773	-0.8059	-0.7274	-0.6569	-0.5871	-0.5195	-0.4532	-0.3879	-0.3238	-0.2609	-0.1994	-0.1391	-0.0777
	0.1026	-0.8270	-0.7472	-0.6720	-0.5995	-0.5287	-0.4596	-0.3926	-0.3270	-0.2629	-0.2005	-0.1396	-0.0776
	0.1362	-0.8527	-0.7725	-0.6933	-0.6167	-0.5424	-0.4703	-0.4003	-0.3323	-0.2663	-0.2024	-0.1403	-0.0773
	0.1807	-0.8742	-0.7967	-0.7166	-0.6375	-0.5601	-0.4846	-0.4113	-0.3403	-0.2717	-0.2054	-0.1412	-0.0767
	0.2389	-0.8769	-0.8037	-0.7310	-0.6535	-0.5759	-0.4992	-0.4257	-0.3501	-0.2784	-0.2092	-0.1420	-0.0749
	0.3129	-0.8330	-0.7778	-0.7139	-0.6452	-0.5738	-0.5011	-0.4278	-0.3546	-0.2820	-0.2105	-0.1404	-0.0701
	0.4017	-0.7130	-0.6789	-0.6347	-0.5836	-0.5271	-0.4666	-0.4029	-0.3369	-0.2690	-0.1998	-0.1296	-0.0584
c.ℓ.	0.5	-0.5023	-0.4340	-0.4050	-0.4478	-0.4134	-0.3729	-0.3269	-0.2760	-0.2208	-0.1617	-0.0991	-0.0350
	0.5983	-0.2280	-0.2451	-0.2513	-0.2487	-0.2383	-0.2200	-0.1964	-0.1661	-0.1304	-0.0898	-0.0444	0.0002
	0.6871	0.0547	0.0171	-0.0092	-0.0265	-0.0360	-0.0386	-0.0352	-0.0269	-0.0143	0.0026	0.0244	0.0398
	0.7611	0.3009	0.2495	0.2100	0.1795	0.1559	0.1375	0.1225	0.1101	0.0999	0.0930	0.0909	0.0744
	0.8193	0.4946	0.4351	0.3884	0.3497	0.3158	0.2842	0.2532	0.2225	0.1929	0.1661	0.1441	0.0993
	0.8638	0.6399	0.5764	0.5257	0.4810	0.4378	0.3941	0.3493	0.3041	0.2596	0.2181	0.1814	0.1153
	0.8974	0.7476	0.6822	0.6285	0.5772	0.5247	0.4704	0.4148	0.3588	0.3038	0.2522	0.2057	0.1249
	0.9227	0.8278	0.7613	0.7033	0.6445	0.5834	0.5207	0.4572	0.3937	0.3316	0.2734	0.2206	0.1305
	0.9420	0.8882	0.8199	0.7559	0.6896	0.6216	0.5527	0.4837	0.4153	0.3486	0.2863	0.2296	0.1338
	0.9569	0.9336	0.8621	0.7912	0.7187	0.6456	0.5726	0.4999	0.4283	0.3588	0.2940	0.2349	0.1356
	0.9685	0.9672	0.8909	0.8138	0.7369	0.6604	0.5846	0.5096	0.4360	0.3648	0.2985	0.2380	0.1367
	0.9777	0.9906	0.9087	0.8276	0.7478	0.6692	0.5916	0.5152	0.4405	0.3683	0.3011	0.2398	0.1374
	0.9851	1.0039	0.9188	0.8356	0.7541	0.6742	0.5956	0.5184	0.4430	0.3703	0.3026	0.2408	0.1377
	0.9910	1.0095	0.9240	0.8398	0.7574	0.6768	0.5977	0.5201	0.4445	0.3713	0.3033	0.2413	0.1379
	0.9959	1.0119	0.9263	0.8417	0.7589	0.6780	0.5986	0.5208	0.4449	0.3717	0.3037	0.2416	0.1380
t.e.	1.0	1.0125	0.9269	0.8422	0.7595	0.6783	0.5988	0.5210	0.4450	0.3718	0.3037	0.2416	0.1380

Table 3

VALUES OF PERTURBATION POTENTIAL × 10 IN PLANE $x^1 = -0.9531\ s$

Body ⟶ ∞

	ξ^3/π \ ξ^2	0	0.0870	0.1823	0.2877	0.4055	0.5390	0.6931	0.8755	1.0986	1.3863	1.7918	2.4849
ℓ.e.	0	-0.8116	-0.7467	-0.6880	-0.5925	-0.5229	-0.4550	-0.3888	-0.3241	-0.2609	-0.1993	-0.1392	-0.0780
	0.0041	-0.8117	-0.7467	-0.6886	-0.5936	-0.5230	-0.4550	-0.3888	-0.3241	-0.2609	-0.1993	-0.1392	-0.0780
	0.0090	-0.8120	-0.7467	-0.6888	-0.5937	-0.5231	-0.4551	-0.3889	-0.3242	-0.2609	-0.1993	-0.1392	-0.0780
	0.0149	-0.8128	-0.7467	-0.6892	-0.5942	-0.5234	-0.4553	-0.3891	-0.3243	-0.2610	-0.1994	-0.1392	-0.0780
	0.0223	-0.8142	-0.7469	-0.6899	-0.5950	-0.5240	-0.4558	-0.3894	-0.3245	-0.2611	-0.1994	-0.1392	-0.0780
	0.0315	-0.8167	-0.7476	-0.6912	-0.5964	-0.5252	-0.4566	-0.3899	-0.3248	-0.2614	-0.1996	-0.1393	-0.0780
	0.0431	-0.8209	-0.7493	-0.6937	-0.5988	-0.5270	-0.4579	-0.3909	-0.3255	-0.2618	-0.1998	-0.1394	-0.0780
	0.0580	-0.8275	-0.7536	-0.6979	-0.6028	-0.5302	-0.4603	-0.3925	-0.3266	-0.2625	-0.2002	-0.1395	-0.0780
	0.0773	-0.8377	-0.7614	-0.6850	-0.6092	-0.5354	-0.4642	-0.3953	-0.3285	-0.2637	-0.2008	-0.1398	-0.0779
	0.1026	-0.8517	-0.7738	-0.6961	-0.6190	-0.5436	-0.4705	-0.3999	-0.3316	-0.2657	-0.2020	-0.1402	-0.0778
	0.1362	-0.8683	-0.7905	-0.7114	-0.6320	-0.5554	-0.4801	-0.4072	-0.3368	-0.2691	-0.2039	-0.1409	-0.0775
	0.1807	-0.8815	-0.8067	-0.7261	-0.6469	-0.5702	-0.4929	-0.4175	-0.3445	-0.2743	-0.2068	-0.1418	-0.0768
	0.2389	-0.8766	-0.8096	-0.7353	-0.6594	-0.5820	-0.5048	-0.4283	-0.3534	-0.2806	-0.2104	-0.1425	-0.0750
	0.3129	-0.8280	-0.7747	-0.7127	-0.6477	-0.5753	-0.5031	-0.4298	-0.3564	-0.2833	-0.2113	-0.1407	-0.0702
	0.4017	-0.7055	-0.6710	-0.6285	-0.5790	-0.5239	-0.4646	-0.4018	-0.3364	-0.2688	-0.1997	-0.1295	-0.0583
c.ℓ.	0.5	-0.4891	-0.4621	-0.4647	-0.4390	-0.4062	-0.3672	-0.3226	-0.2729	-0.2187	-0.1604	-0.0984	-0.0348
	0.5983	-0.2113	-0.2297	-0.2575	-0.2566	-0.2278	-0.2119	-0.1894	-0.1608	-0.1267	-0.0875	-0.0433	0.0005
	0.6871	0.0749	0.0357	0.0075	-0.0117	-0.0232	-0.0279	-0.0268	-0.0206	-0.0100	0.0052	0.0257	0.0402
	0.7611	0.3248	0.2710	0.2291	0.1959	0.1695	0.1482	0.1306	0.1157	0.1036	0.0952	0.0919	0.0746
	0.8193	0.5220	0.4591	0.4086	0.3659	0.3281	0.2928	0.2589	0.2262	0.1951	0.1674	0.1447	0.0994
	0.8638	0.6702	0.6013	0.5446	0.4940	0.4459	0.3987	0.3518	0.3054	0.2602	0.2185	0.1816	0.1152
	0.8974	0.7783	0.7045	0.6418	0.5836	0.5268	0.4703	0.4140	0.3579	0.3031	0.2519	0.2055	0.1247
	0.9227	0.8524	0.7744	0.7065	0.6423	0.5793	0.5165	0.4537	0.3912	0.3300	0.2727	0.2202	0.1302
	0.9420	0.8959	0.8172	0.7469	0.6794	0.6124	0.5454	0.4783	0.4116	0.3464	0.2852	0.2290	0.1335
	0.9569	0.9266	0.8417	0.7715	0.7023	0.6329	0.5631	0.4932	0.4239	0.3562	0.2927	0.2343	0.1353
	0.9685	0.9258	0.8558	0.7864	0.7162	0.6452	0.5737	0.5021	0.4311	0.3620	0.2971	0.2373	0.1364
	0.9777	0.9302	0.8646	0.7953	0.7245	0.6525	0.5799	0.5075	0.4353	0.3653	0.2996	0.2391	0.1370
	0.9851	0.9325	0.8690	0.8004	0.7291	0.6566	0.5834	0.5102	0.4377	0.3672	0.3010	0.2401	0.1374
	0.9910	0.9333	0.8716	0.8031	0.7316	0.6587	0.5852	0.5117	0.4389	0.3681	0.3018	0.2406	0.1376
	0.9959	0.9337	0.8723	0.8043	0.7327	0.6597	0.5860	0.5124	0.4395	0.3686	0.3021	0.2408	0.1376
t.e.	1.0	0.9338	0.8731	0.8046	0.7330	0.6599	0.5862	0.5125	0.4396	0.3687	0.3022	0.2408	0.1377

Table 4

VALUES OF PERTURBATION POTENTIAL × 10 IN PLANE $x^1 = -0.9160$ s

Body → ∞

	ξ^3/π \ ξ^2	0	0.0870	0.1823	0.2877	0.4055	0.5390	0.6931	0.8755	1.0986	1.3863	1.7918	2.4849
l.e.	0	-0.9151	-0.8602	-0.7902	-0.7068	-0.6123	-0.5168	-0.4287	-0.3488	-0.2752	-0.2067	-0.1423	-0.0789
	0.0041	-0.9151	-0.8601	-0.7901	-0.7067	-0.6123	-0.5168	-0.4288	-0.3488	-0.2752	-0.2067	-0.1423	-0.0789
	0.0090	-0.9152	-0.8597	-0.7897	-0.7065	-0.6122	-0.5168	-0.4288	-0.3489	-0.2753	-0.2067	-0.1423	-0.0789
	0.0149	-0.9153	-0.8588	-0.7889	-0.7060	-0.6121	-0.5169	-0.4289	-0.3490	-0.2753	-0.2068	-0.1423	-0.0789
	0.0223	-0.9155	-0.8572	-0.7874	-0.7050	-0.6118	-0.5170	-0.4292	-0.3491	-0.2754	-0.2068	-0.1423	-0.0789
	0.0315	-0.9160	-0.8551	-0.7851	-0.7035	-0.6114	-0.5173	-0.4296	-0.3495	-0.2757	-0.2069	-0.1424	-0.0789
	0.0431	-0.9167	-0.8524	-0.7820	-0.7013	-0.6108	-0.5178	-0.4303	-0.3500	-0.2760	-0.2071	-0.1424	-0.0789
	0.0580	-0.9178	-0.8496	-0.7782	-0.6986	-0.6101	-0.5186	-0.4314	-0.3510	-0.2767	-0.2075	-0.1426	-0.0788
	0.0773	-0.9191	-0.8471	-0.7744	-0.6956	-0.6094	-0.5199	-0.4334	-0.3527	-0.2778	-0.2082	-0.1428	-0.0788
	0.1026	-0.9200	-0.8453	-0.7711	-0.6929	-0.6092	-0.5221	-0.4364	-0.3553	-0.2797	-0.2092	-0.1432	-0.0786
	0.1362	-0.9185	-0.8434	-0.7685	-0.6911	-0.6096	-0.5252	-0.4407	-0.3594	-0.2827	-0.2110	-0.1438	-0.0783
	0.1807	-0.9095	-0.8375	-0.7641	-0.6884	-0.6096	-0.5282	-0.4457	-0.3646	-0.2869	-0.2135	-0.1446	-0.0775
	0.2389	-0.8808	-0.8166	-0.7488	-0.6777	-0.6035	-0.5266	-0.4478	-0.3687	-0.2909	-0.2161	-0.1449	-0.0755
	0.3129	-0.8089	-0.7587	-0.7028	-0.6420	-0.5770	-0.5084	-0.4370	-0.3634	-0.2889	-0.2147	-0.1421	-0.0703
	0.4017	-0.6639	-0.6345	-0.5978	-0.5548	-0.5060	-0.4524	-0.3942	-0.3322	-0.2668	-0.1988	-0.1289	-0.0579
c.l.	0.5	-0.4318	-0.4279	-0.4161	-0.3969	-0.3709	-0.3386	-0.3005	-0.2568	-0.2078	-0.1539	-0.0951	-0.0336
	0.5983	-0.1384	-0.1603	-0.1740	-0.1799	-0.1786	-0.1706	-0.1561	-0.1355	-0.1091	-0.0766	-0.0377	0.0022
	0.6871	0.1615	0.1179	0.0826	0.0549	0.0342	0.0198	0.0110	0.0075	0.0093	0.0171	0.0317	0.0417
	0.7611	0.4212	0.3612	0.3092	0.2644	0.2257	0.1924	0.1636	0.1391	0.1191	0.1046	0.0967	0.0756
	0.8193	0.6160	0.5438	0.4793	0.4217	0.3699	0.3228	0.2796	0.2399	0.2040	0.1729	0.1474	0.0996
	0.8638	0.7354	0.6567	0.5862	0.5226	0.4642	0.4097	0.3582	0.3090	0.2625	0.2202	0.1824	0.1147
	0.8974	0.7934	0.7154	0.6461	0.5824	0.5224	0.4646	0.4084	0.3534	0.3003	0.2506	0.2048	0.1238
	0.9227	0.8202	0.7466	0.6807	0.6186	0.5582	0.4987	0.4396	0.3809	0.3236	0.2694	0.2185	0.1291
	0.9420	0.8333	0.7651	0.7023	0.6412	0.5804	0.5196	0.4586	0.3976	0.3377	0.2807	0.2267	0.1321
	0.9569	0.8400	0.7770	0.7163	0.6555	0.5942	0.5323	0.4700	0.4076	0.3460	0.2874	0.2315	0.1339
	0.9685	0.8436	0.7849	0.7253	0.6644	0.6025	0.5399	0.4768	0.4135	0.3509	0.2913	0.2343	0.1349
	0.9777	0.8456	0.7901	0.7310	0.6698	0.6074	0.5443	0.4807	0.4169	0.3538	0.2935	0.2360	0.1355
	0.9851	0.8466	0.7933	0.7343	0.6729	0.6102	0.5468	0.4829	0.4188	0.3553	0.2948	0.2369	0.1358
	0.9910	0.8472	0.7950	0.7362	0.6745	0.6117	0.5481	0.4840	0.4197	0.3562	0.2955	0.2373	0.1360
	0.9959	0.8474	0.7959	0.7370	0.6753	0.6123	0.5487	0.4845	0.4202	0.3565	0.2957	0.2375	0.1361
t.e.	1.0	0.8474	0.7961	0.7372	0.6755	0.6125	0.5489	0.4847	0.4203	0.3566	0.2958	0.2376	0.1361

Table 5

VALUES OF PERTURBATION POTENTIAL × 10 IN PLANE $x^1 = 0$ (CENTER SECTION)

Body → ∞

	ξ^3/π \ ξ^2	0	0.0870	0.1823	0.2877	0.4055	0.5390	0.6931	0.8755	1. 986	1.3863	1.7918	2.4849
l.e.	0	-0.8582	-0.8091	-0.7519	-0.6909	-0.6282	-0.5651	-0.5024	-0.4408	-0.3799	-0.3140	-0.2219	-0.1050
	0.0041	-0.8582	-0.8089	-0.7517	-0.6907	-0.6281	-0.5650	-0.5023	-0.4408	-0.3799	-0.3139	-0.2219	-0.1050
	0.0090	-0.8580	-0.8082	-0.7510	-0.6901	-0.6276	-0.5646	-0.5020	-0.4405	-0.3796	-0.3138	-0.2218	-0.1050
	0.0149	-0.8576	-0.8067	-0.7495	-0.6888	-0.6265	-0.5636	-0.5012	-0.4399	-0.3792	-0.3134	-0.2217	-0.1049
	0.0223	-0.8569	-0.8040	-0.7466	-0.6863	-0.6244	-0.5619	-0.4998	-0.4387	-0.3782	-0.3128	-0.2213	-0.1049
	0.0315	-0.8555	-0.7997	-0.7420	-0.6820	-0.6207	-0.5588	-0.4972	-0.4366	-0.3765	-0.3115	-0.2208	-0.1047
	0.0431	-0.8530	-0.7933	-0.7348	-0.6752	-0.6145	-0.5535	-0.4927	-0.4329	-0.3736	-0.3094	-0.2197	-0.1045
	0.0580	-0.8484	-0.7842	-0.7241	-0.6645	-0.6048	-0.5448	-0.4853	-0.4267	-0.3686	-0.3058	-0.2180	-0.1040
	0.0773	-0.8399	-0.7712	-0.7087	-0.6487	-0.5896	-0.5311	-0.4733	-0.4165	-0.3603	-0.2996	-0.2149	-0.1033
	0.1026	-0.8240	-0.7516	-0.6864	-0.6254	-0.5669	-0.5099	-0.4542	-0.4000	-0.3466	-0.2893	-0.2096	-0.1018
	0.1362	-0.7941	-0.7204	-0.6554	-0.5915	-0.5333	-0.4779	-0.4249	-0.3741	-0.3248	-0.2725	-0.2005	-0.0992
	0.1807	-0.7398	-0.6684	-0.6021	-0.5409	-0.4841	-0.4311	-0.3815	-0.3351	-0.2912	-0.2461	-0.1851	-0.0943
	0.2389	-0.6450	-0.5813	-0.5209	-0.4643	-0.4119	-0.3637	-0.3195	-0.2792	-0.2424	-0.2064	-0.1598	-0.0847
	0.3129	-0.4915	-0.4424	-0.3949	-0.3499	-0.3079	-0.2693	-0.2344	-0.2034	-0.1761	-0.1510	-0.1205	-0.0671
	0.4017	-0.2702	-0.2431	-0.2166	-0.1912	-0.1673	-0.1452	-0.1254	-0.1081	-0.0933	-0.0803	-0.0656	-0.0381
c.l.	0.5	-0.0000	-0.0000	-0.0000	-0.0000	-0.0000	-0.0000	-0.0000	-0.0000	-0.0000	-0.0000	-0.0000	-0.0000
	0.5983	0.2702	0.2431	0.2166	0.1912	0.1673	0.1452	0.1254	0.1081	0.0933	0.0803	0.0656	0.0381
	0.6871	0.4915	0.4424	0.3949	0.3499	0.3079	0.2693	0.2344	0.2034	0.1761	0.1510	0.1205	0.0671
	0.7611	0.6450	0.5813	0.5209	0.4643	0.4119	0.3637	0.3195	0.2792	0.2424	0.2064	0.1598	0.0847
	0.8193	0.7398	0.6684	0.6021	0.5409	0.4841	0.4311	0.3815	0.3351	0.2912	0.2461	0.1851	0.0943
	0.8638	0.7941	0.7204	0.6534	0.5915	0.5333	0.4779	0.4249	0.3741	0.3248	0.2725	0.2005	0.0992
	0.8974	0.8240	0.7516	0.6864	0.6254	0.5669	0.5099	0.4542	0.4000	0.3466	0.2893	0.2096	0.1018
	0.9227	0.8399	0.7712	0.7087	0.6487	0.5896	0.5311	0.4733	0.4165	0.3603	0.2996	0.2149	0.1033
	0.9420	0.8484	0.7842	0.7241	0.6645	0.6048	0.5448	0.4853	0.4267	0.3686	0.3058	0.2180	0.1040
	0.9569	0.8530	0.7933	0.7348	0.6752	0.6145	0.5535	0.4927	0.4329	0.3736	0.3094	0.2197	0.1045
	0.9685	0.8555	0.7997	0.7420	0.6821	0.6207	0.5588	0.4972	0.4366	0.3765	0.3115	0.2208	0.1047
	0.9777	0.8569	0.8040	0.7467	0.6863	0.6244	0.5619	0.4998	0.4387	0.3782	0.3128	0.2213	0.1049
	0.9851	0.8577	0.8067	0.7495	0.6888	0.6265	0.5637	0.5012	0.4399	0.3792	0.3134	0.2217	0.1049
	0.9910	0.8580	0.8083	0.7510	0.6902	0.6276	0.5646	0.5020	0.4405	0.3797	0.3138	0.2218	0.1050
	0.9959	0.8582	0.8090	0.7517	0.6908	0.6281	0.5650	0.5023	0.4408	0.3799	0.3140	0.2219	0.1050
t.e.	1.0	0.8582	0.8092	0.7519	0.6909	0.6282	0.5651	0.5024	0.4409	0.3800	0.3140	0.2219	0.1050

SYMBOLS

a	local speed of sound column matrix in Appendix B
$\underline{a}_i$	base vector
$\underline{a}^i$	normal vector
a_i	element of matrix a
A	$\left\|\frac{df}{d\zeta}\right\|$
b_i, c_i, d_i	elements of matrix T
c	semi-chord of ellipse
$\underline{c}_i$	cartesian unit base vector
C,D	real, imaginary parts of $\frac{df}{d\zeta}$
E,F	real, imaginary parts of $\frac{d^2f}{d\zeta^2}$
f	mapping functions from x^i to ξ^i
g_{ij}	covariant metric tensor of order 2
g^{ij}	contravariant metric tensor of order 2
h_i	mesh-length in η^i
J	Jacobian of the transformation from x^i to ξ^i
L,M,N	mesh sizes in η^3, η^2, η^1, respectively
M_∞	freestream Mach number
M_{max}	maximum Mach number
P_i	$= \frac{d\eta^i}{d\xi^i}$
q	fluid speed
Q^i	see equation (3-7)
r_i	element of matrix R
R	see equation (3-10) lower triangular matrix in Appendix B
s	semi-span
s_i	element of matrix R
S	see equation (3-10)
t^i_j	$= \frac{\partial x^i}{\partial \xi^j}$
T	see equation (3-10) tridiagonal matrix in Appendix B
u	column matrix in Appendix B

SYMBOLS (concluded)

U	upper diagonal matrix in Appendix B
U_∞	freestream velocity
$\underline{v}$	arbitrary vector
$\underline{V}$	velocity vector
V_i	covariant component of $\underline{V}$
V^i	contravariant component of $\underline{V}$
x^i	cartesian coordinates
x,y,z	cartesian coordinates equivalent to $(-x^2,x^1,x^3)$
Y_i	$= V^i$
z	column matrix in Appendix B
α	parameter of the transformation from ξ^1 to η^1
β	parameter of the transformation from ξ^3 to η^3
γ	ratio of specific heats
Γ	see equation (2-12)
δ_{ij},δ^i_j	Kronecker delta symbols $= 0$ if $i \neq j$; $= 1$ if $i = j$
Δ	see equation (2-12)
$\varepsilon_{ijk},\varepsilon^{ijk}$	see equation (A-2)
ζ	$= \xi^2 + i\xi^3$
η^i	general coordinate used for the solution
Λ	angle of sweep of the centre chord
μ	$= \tan \Lambda$
ξ^i	general coordinate (intermediate)
τ	thickness/chord ratio
ϕ	perturbation velocity potential
ϕ_i,ϕ_{ij}	$\frac{\partial \phi}{\partial \eta^i}, \frac{\partial^2 \phi}{\partial \eta^i \partial \eta^j}$
$\phi_{i,j,k}$	value of ϕ at grid point (i,j,k)
Φ	total velocity potential
Φ_∞	freestream velocity potential
ω	relaxation parameter

REFERENCES

No.	Author	Title, etc
1	C.C.L. Sells	Plane subcritical flow past a lifting aerofoil. Proc. Roy. Soc., A, 308, 377-401 (1968)
2	E.M. Murman J.D. Cole	Calculation of plane steady transonic flows. AIAA Jnl., Vol 9, p 114, January 1971
3	J.L. Steger H. Lomax	Transonic flow about two-dimensional airfoils by relaxation procedures. AIAA Jnl., Vol 10, p 49, January 1972
4	F. Bauer P. Garabadian D. Korn	A theory of supercritical wing sections. Springer-Verlag (1972)
5	P.W. Duck	The numerical calculation of steady inviscid supercritical flow past ellipsoids without circulation. ARC R & M No.3794 (1977)
6	A. Jameson	Iterative solution of transonic flows over airfoils and wings, including flows at Mach 1. Comm. Pure Appl. Maths., Vol 27, p 283, May 1974
7	K.W. Mangler J.C. Murray	Systems of coordinates suitable for the numerical calculation of three-dimensional flow fields. ARC CP No.1325 (1975)

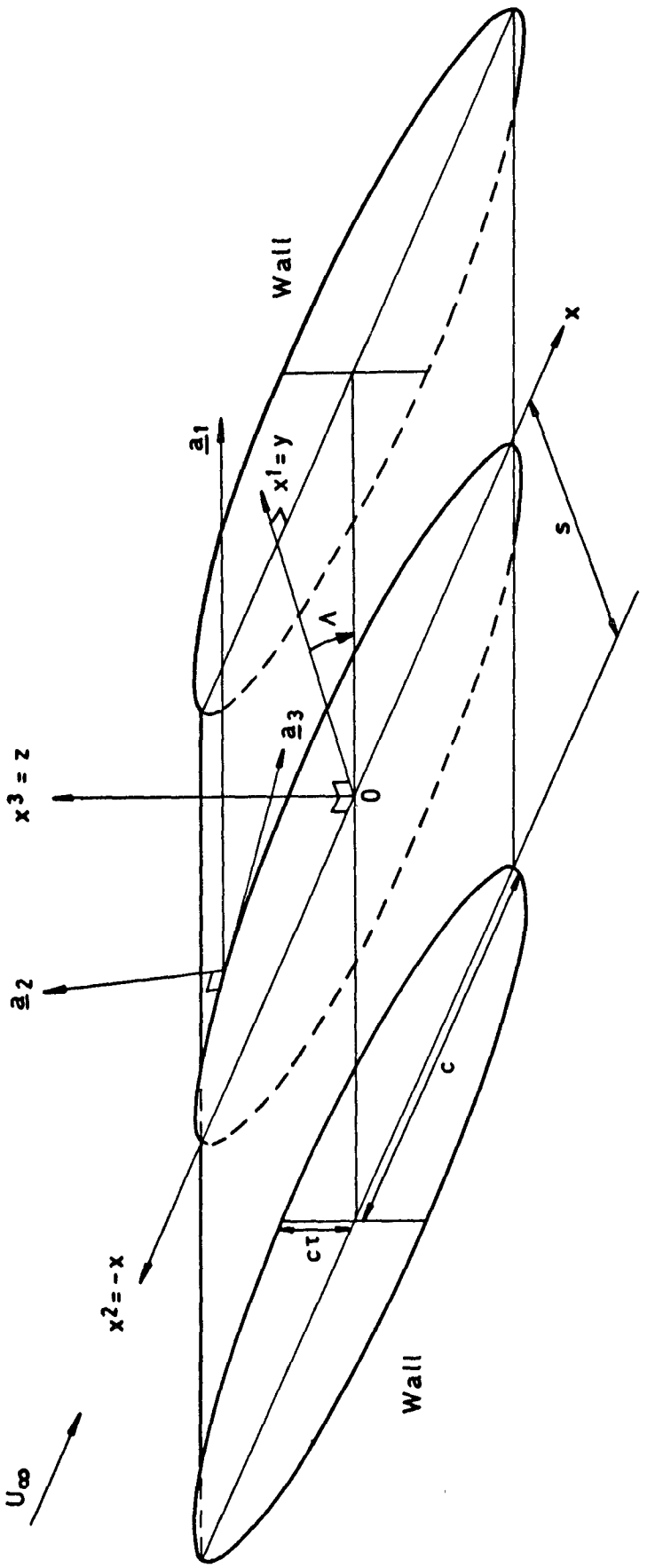

Fig 1 Flow past a swept elliptic cylinder between walls

Fig 2

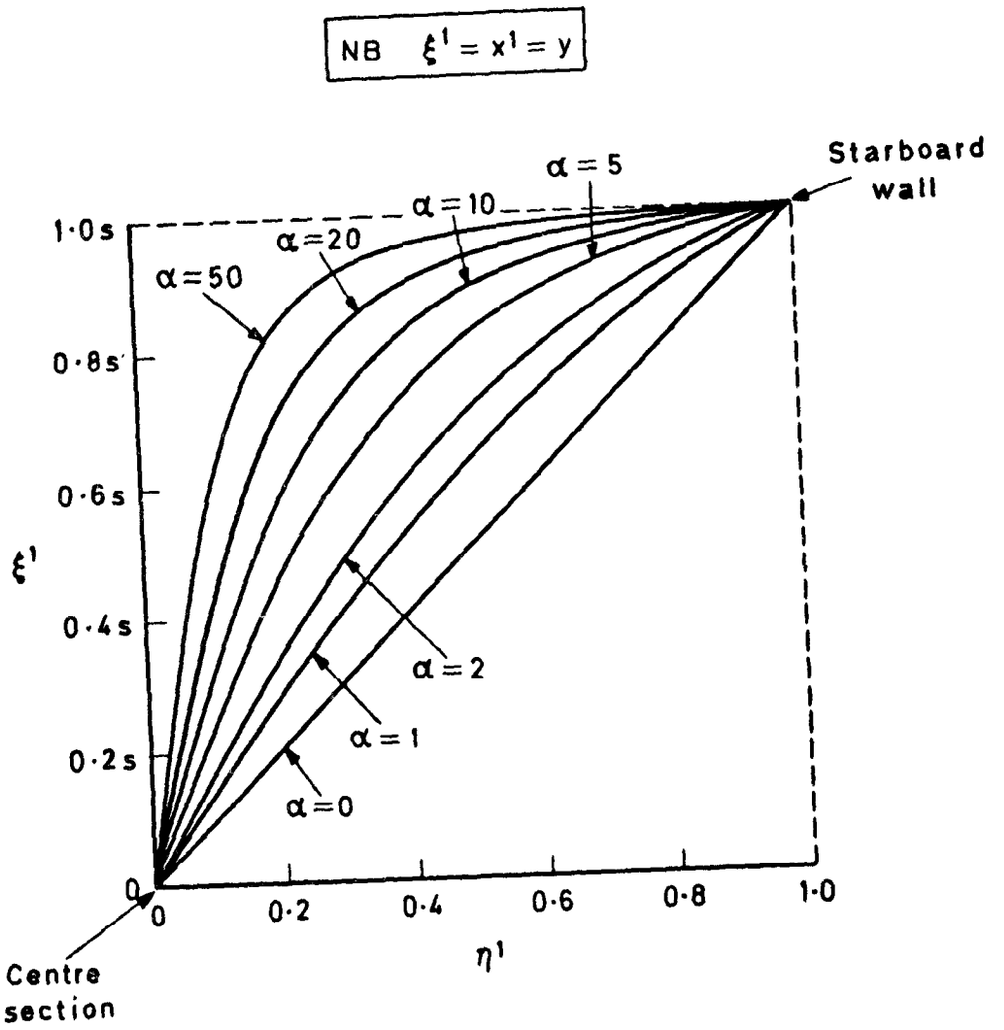

Fig 2 The variation of the η^1–transformation (equation (2-10)) with α

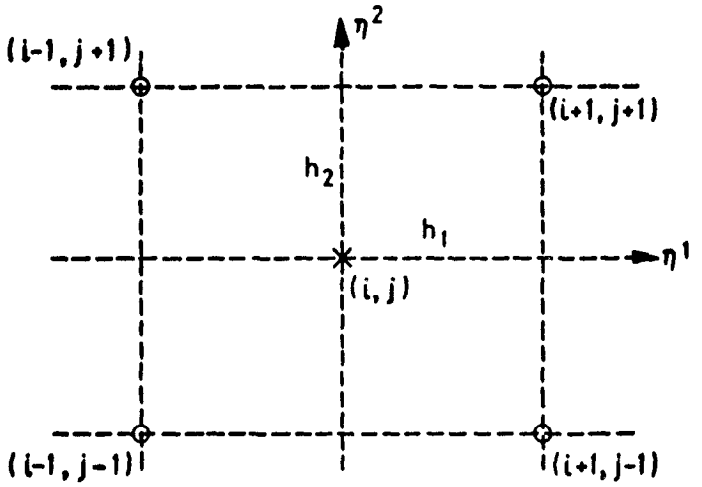

$$\frac{\partial^2\phi}{\partial\eta^1\partial\eta^2} = (\phi_{i+1,j+1} - \phi_{i+1,j-1} - \phi_{i-1,j+1} + \phi_{i-1,j-1})/4h_1h_2 + O(h_1^2 + h_2^2)$$

i Normal differencing

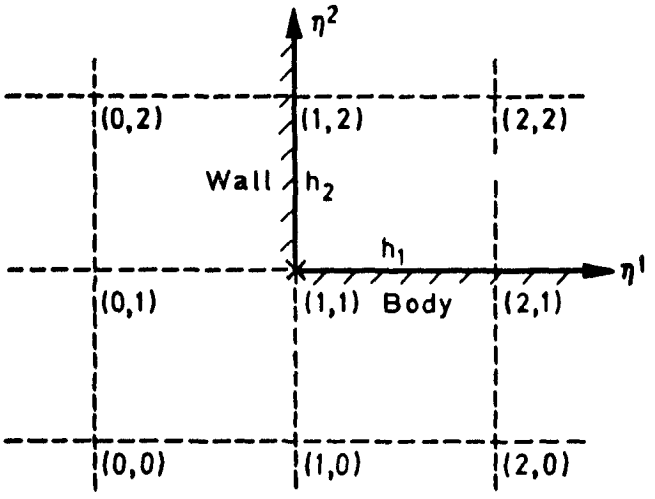

$\phi_{i-1,j-1} \equiv \phi_{0,0}$ is unobtainable from boundary conditions

$$\frac{\partial^2\phi}{\partial\eta^1\partial\eta^2} = -\left[2\phi_{1,1} + \phi_{2,0} + \phi_{0,2} - \phi_{1,2} - \phi_{1,0} - \phi_{2,1} - \phi_{0,1}\right]/2h_1h_2 + O(h_1^2 + h_2^2)$$

ii Differencing in corner

Fig 3 Difference schemes for $\frac{\partial^2\phi}{\partial\eta^1\partial\eta^2}$

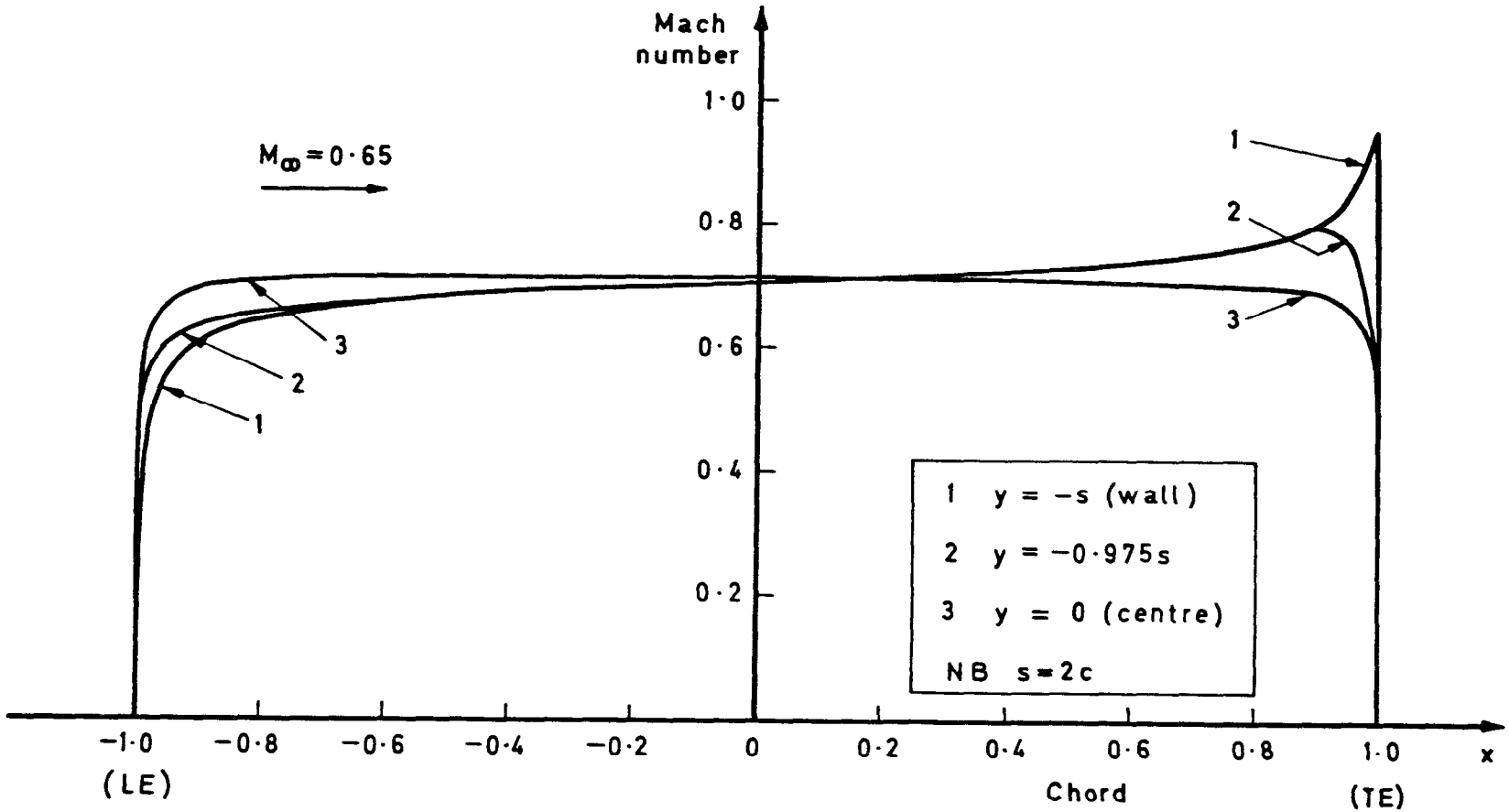

Fig 4 Mach number distribution in sectional planes for flow past a 10% ellipse swept at 45° (41 x 32 x 41 grid)

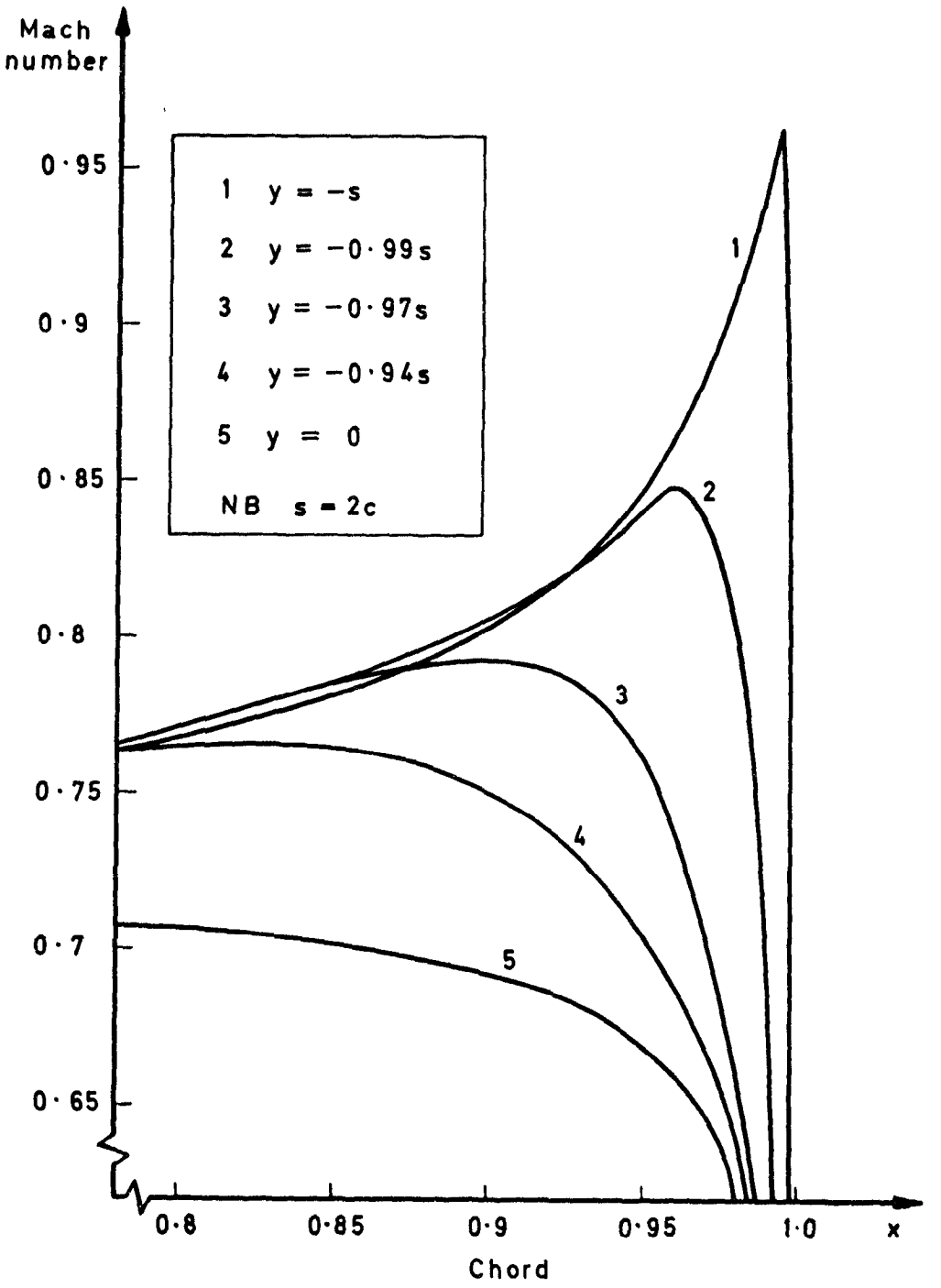

Fig 5 Enlargement of the trailing-edge region of Fig 4

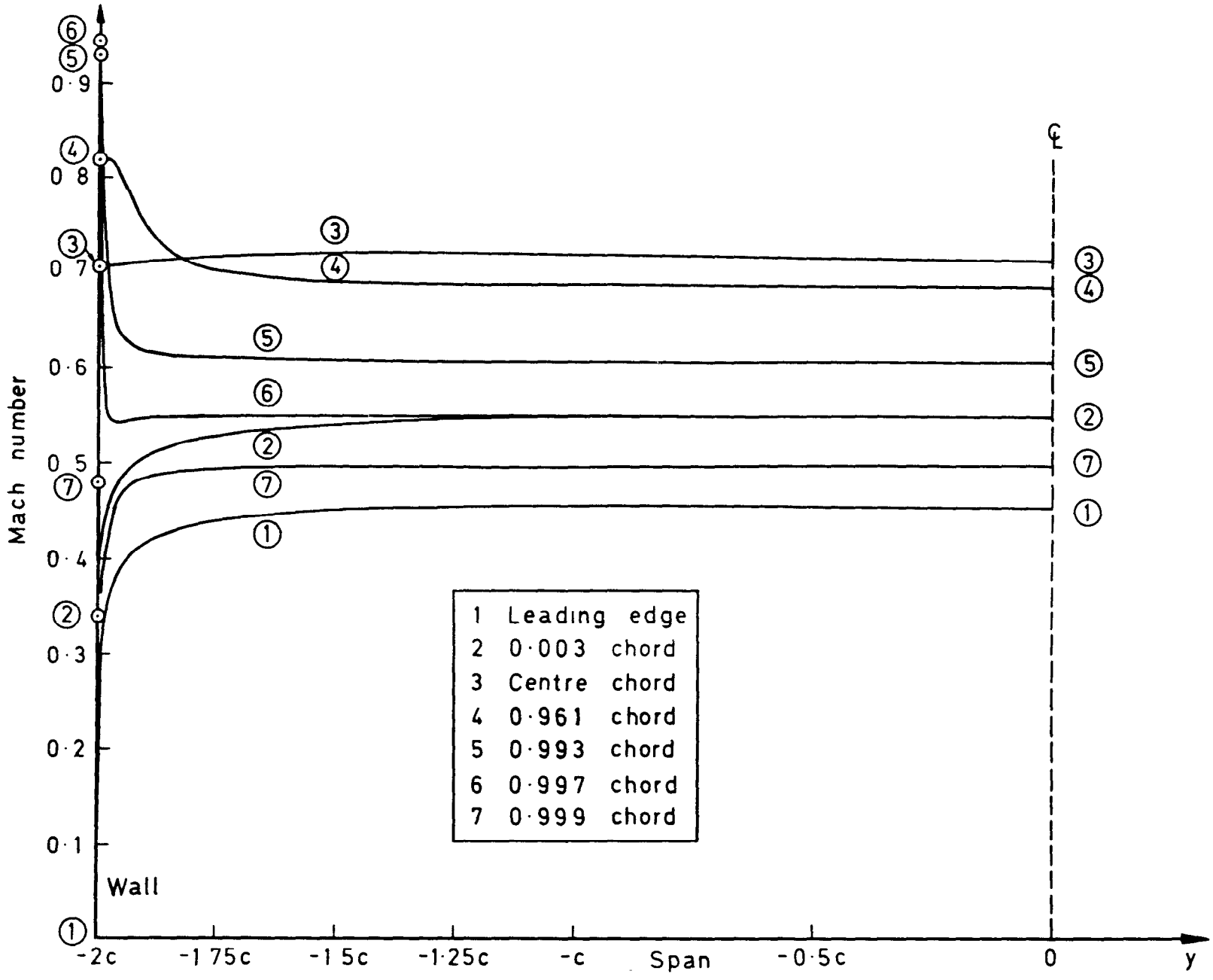

Fig 6 Variation of Mach number in constant-chord sections (flow as in Fig 4)

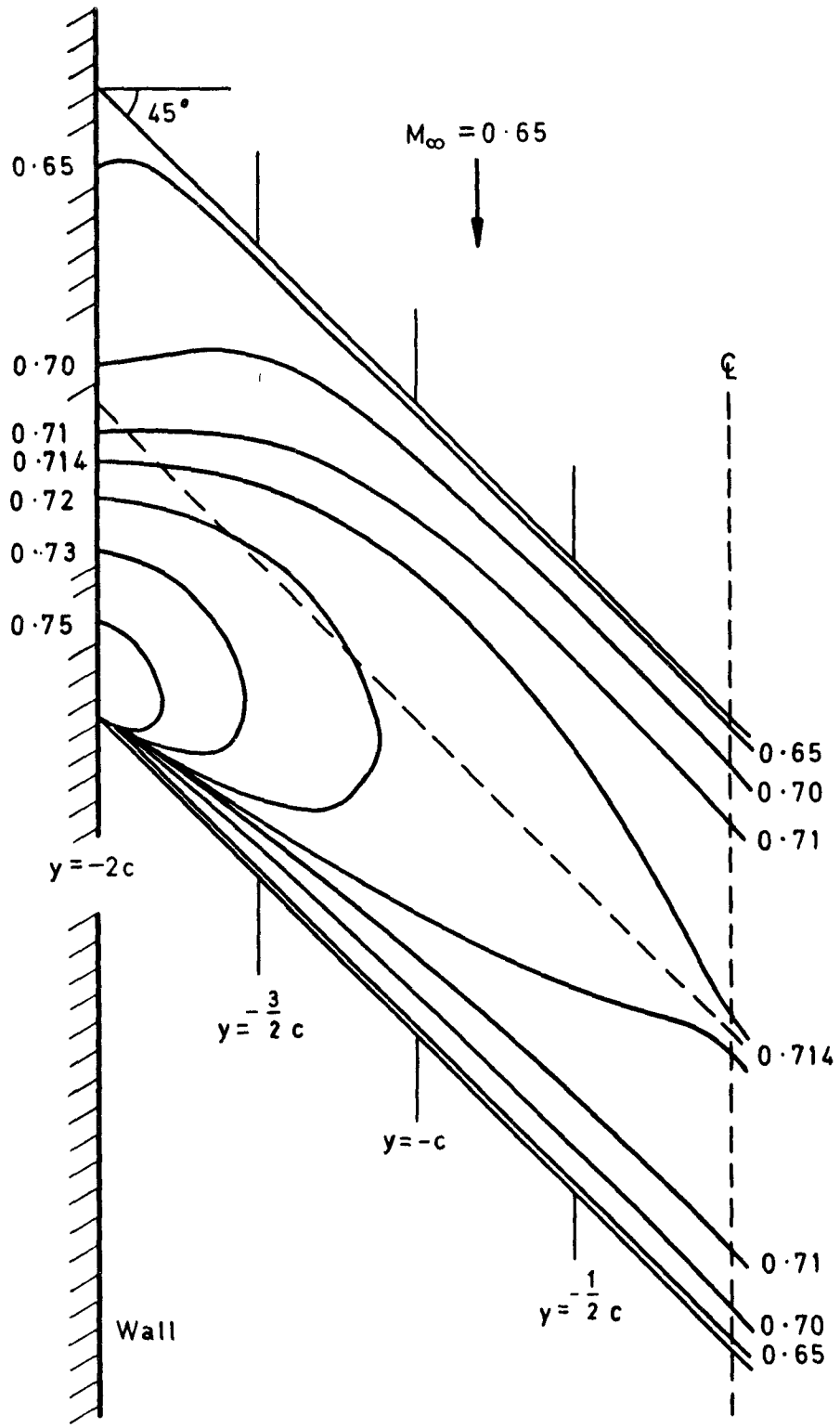

Fig 7 Mach number contours on the wing surface

Fig 8

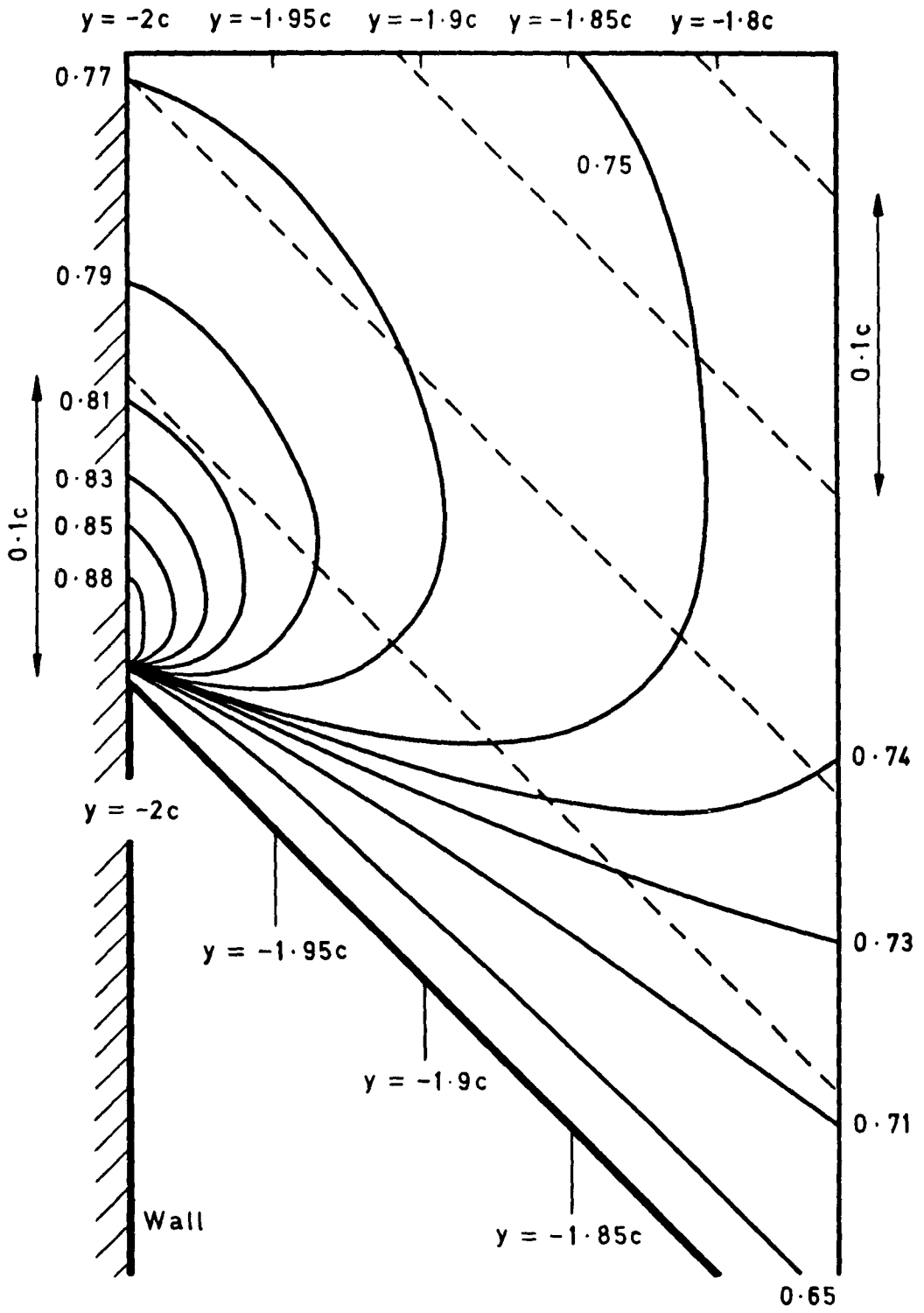

Fig 8 Enlargement of trailing-edge region of Fig 7

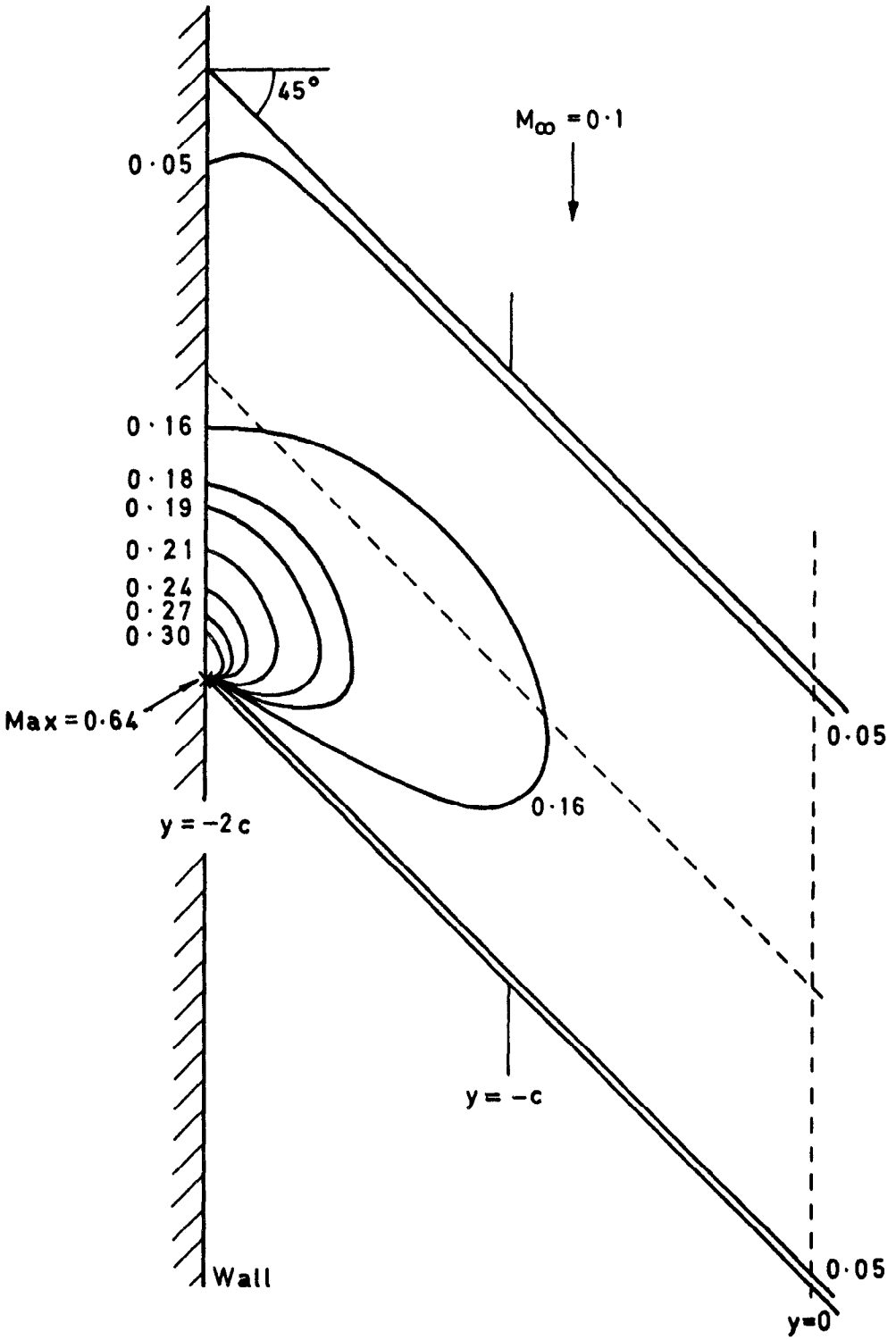

Fig 9a Shows isobars on the wing for increasing freestream Mach number (values shown are $-C_p$)

Fig 9b

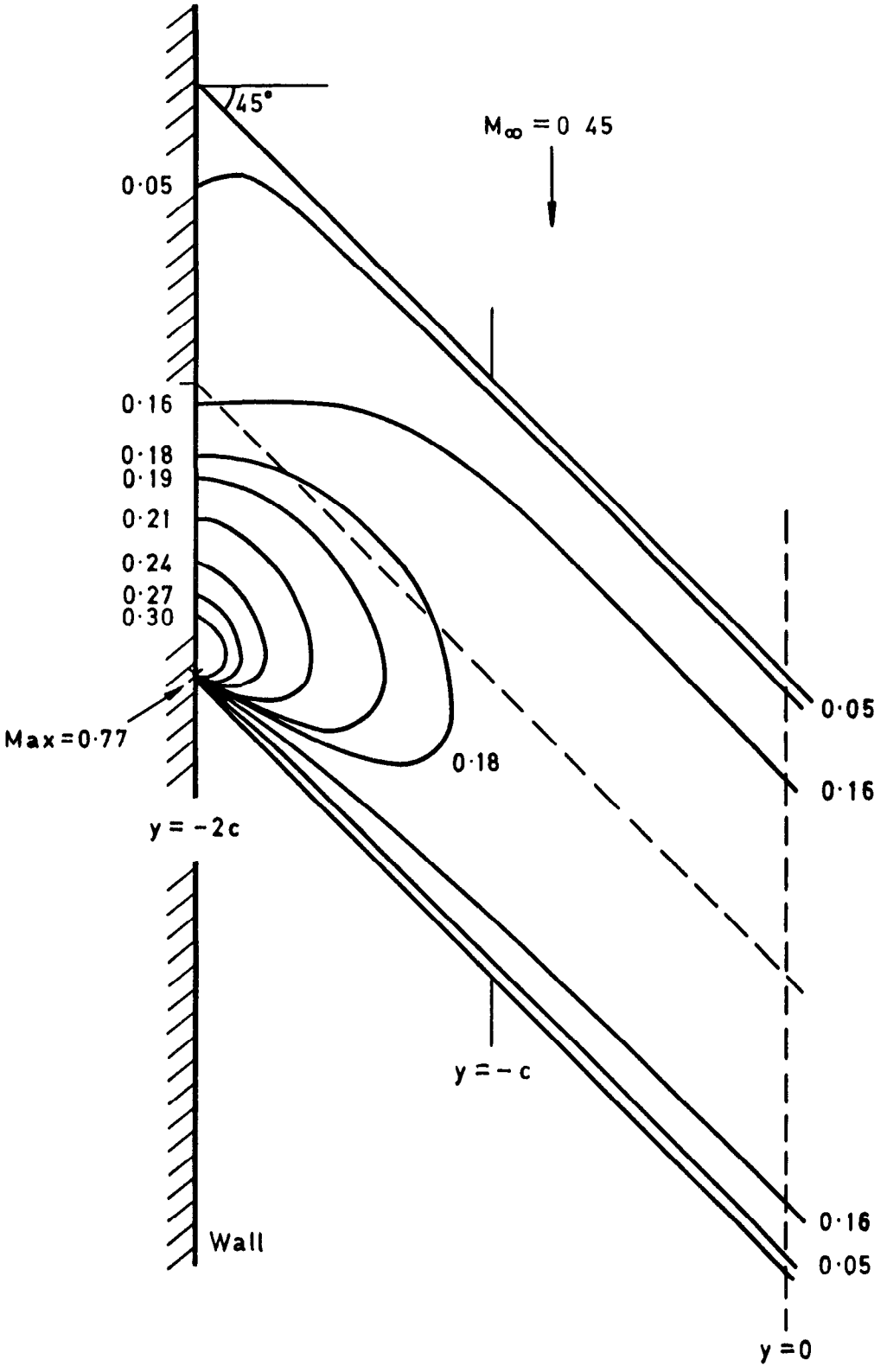

Fig 9b Shows isobars on the wing for increasing freestream Mach number (values shown are $-C_p$)

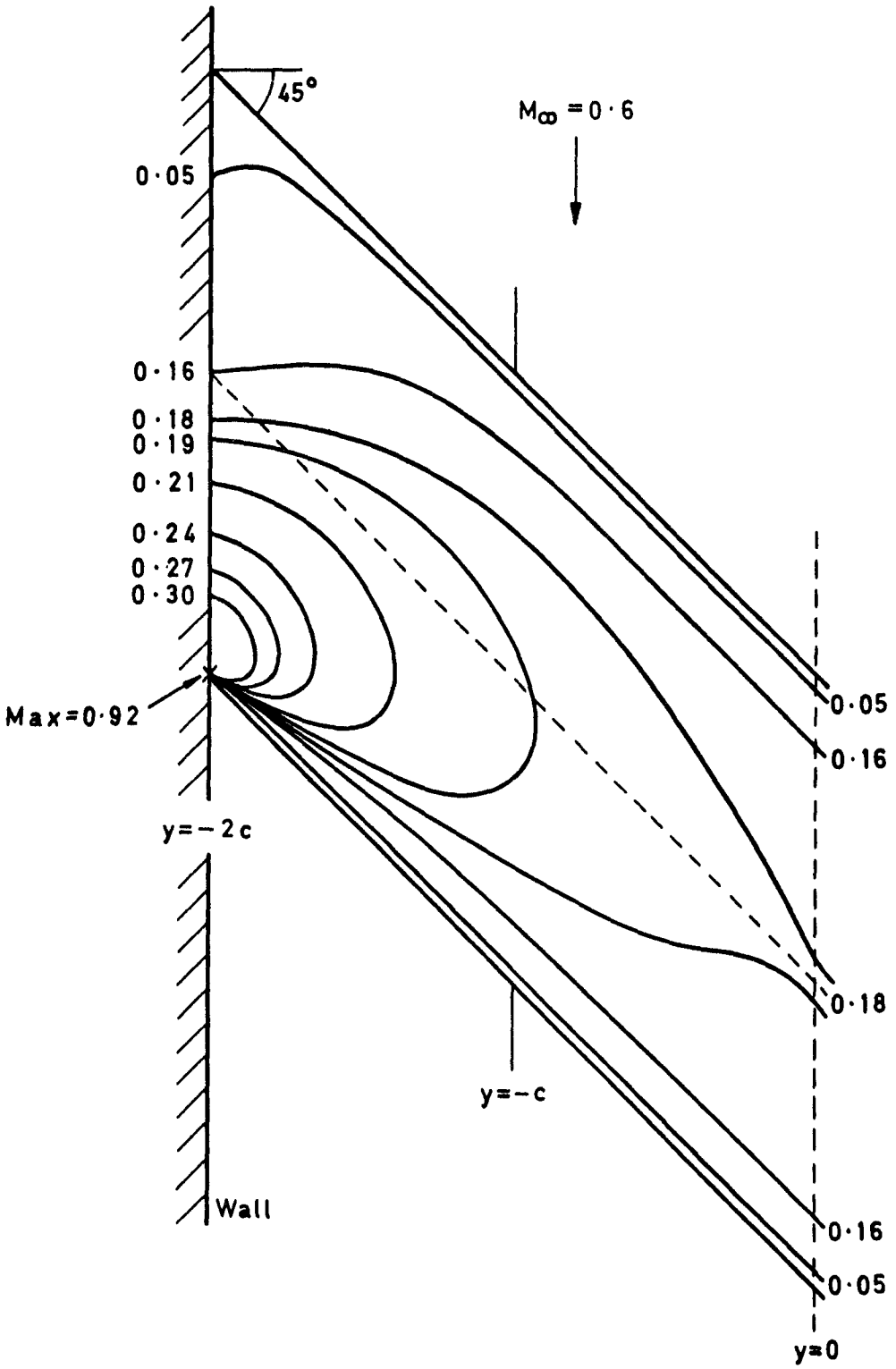

Fig 9c Shows isobars on the wing for increasing freestream Mach number (values shown are $-C_p$)

Fig 9d

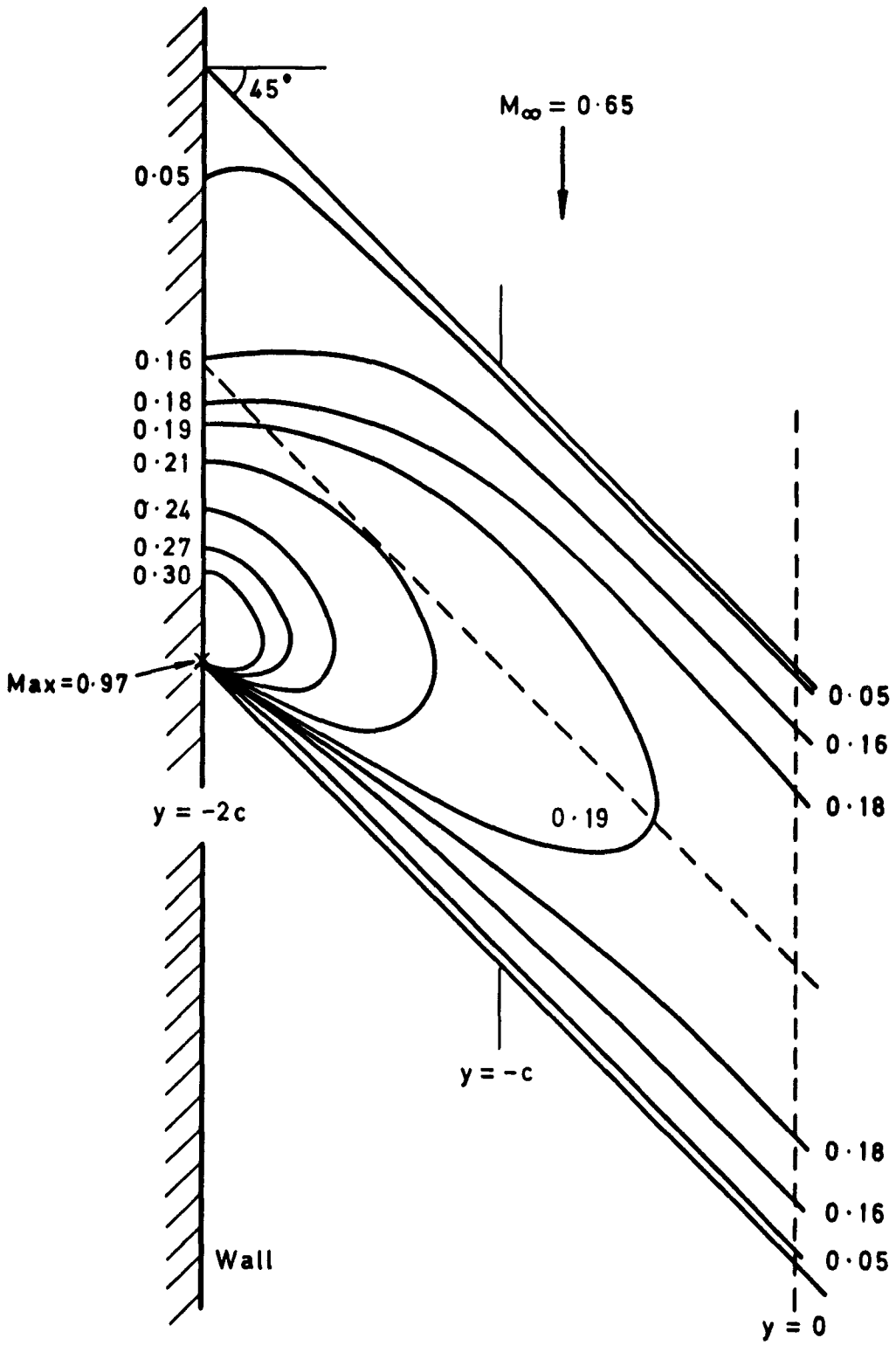

Fig 9d Shows isobars on the wing for increasing freestream Mach number (values shown are $-C_p$)

Printed in England for Her Majesty's Stationery Office by the Royal Aircraft Establishment, Farnborough. Dd. 587483 K4 3/79.

ARC CP No.1393
June 1976

G.J. Clapworthy

533.6.011.34 :
533.692.7 :
533.693.1 :
533.6.071.4 ·
517.949

THE CALCULATION, BY A FINITE-DIFFERENCE METHOD, OF SUBCRITICAL FLOW WITHOUT CIRCULATION PAST A SWEPT ELLIPTIC CYLINDER BETWEEN WALLS

The full equations of motion are expressed in coordinates defined by the body shape and the exact body surface boundary conditions are applied. The flow equations are expressed in terms of the velocity potential and are solved by finite-difference methods. For accuracy, further transformations are necessary to concentrate the grid points in regions of greatest variation in potential.

Mach number and pressure distributions are presented for typical cases.

ARC CP No.1393
June 1976

G.J. Clapworthy

533.6.011.34 :
533.692.7 .
533.693.1 :
533.6.071.4 :
517.949

THE CALCULATION, BY A FINITE-DIFFERENCE METHOD, OF SUBCRITICAL FLOW WITHOUT CIRCULATION PAST A SWEPT ELLIPTIC CYLINDER BETWEEN WALLS

The full equations of motion are expressed in coordinates defined by the body shape and the exact body surface boundary conditions are applied. The flow equations are expressed in terms of the velocity potential and are solved by finite-difference methods. For accuracy, further transformations are necessary to concentrate the grid points in regions of greatest variation in potential.

Mach number and pressure distributions are presented for typical cases.

First published 1979

HER MAJESTY'S STATIONERY OFFICE

Government Bookshops
49 High Holborn, London WC1V 6HB
13a Castle Street, Edinburgh EH2 3AR
41 The Hayes, Cardiff CF1 1JW
Brazennose Street, Manchester M60 8AS
Southey House, Wine Street, Bristol BS1 2BQ
258 Broad Street, Birmingham B1 2HE
80 Chichester Street, Belfast BT1 4JY

Government Publications are also available through booksellers

C.P. No.1393
ISBN 011471139 9